Appl Phys A (2012) 106:937–940
DOI 10.1007/s00339-011-6713-5

Applied Physics A
Materials Science & Processing

Structural, optical and electrical properties of cubic AlN films deposited by laser molecular beam epitaxy

Yuechun Fu · Xuefei Li · Yunyun Wang · Huan He · Xiaoming Shen

Received: 27 May 2011 / Accepted: 29 November 2011 / Published online: 15 December 2011
© Springer-Verlag 2011

Abstract Cubic AlN films were successfully deposited on TiN buffered Si (100) substrates by a laser molecular beam epitaxy (LMBE) technique, and their crystal structure and optical and electrical properties were studied. The results indicate that cubic AlN films show the NaCl-type structure with a (200) preferred orientation, and the lattice parameter is determined to be 0.4027 nm. The Fourier transform infrared (FTIR) pattern of the cubic AlN film displays sharp absorption peaks at 668 cm^{-1} and 951 cm^{-1}, corresponding to the transverse and longitudinal optical vibration modes. Ellipsometric measurements evidence a refractive index of 1.66–1.71 and an extinction coefficient of about zero for the cubic AlN film in the visible range. Capacitance–voltage (C–V) traces of the metal–insulator–semiconductor (MIS) device exhibit that the cubic AlN film has a dielectric constant of 8.1, and hysteresis in the C–V traces indicates a significant number of charge traps in the film.

1 Introduction

The III–V semiconductor AlN having the hexagonal wurtzite structure has been extensively studied for its stability and excellent properties. Cubic AlN (zinc-blende or NaCl structure) is expected to have decreased phonon scattering and therefore higher ballistic electron velocities, thermal conductivity and acoustic velocity due to its higher symmetry [1]. However, the synthesis of cubic AlN is more difficult than hexagonal AlN because it is a metastable phase [2–4]. Hexagonal inclusions and a comparably rough surface impede so far a reliable experimental determination of optical and electrical properties of cubic AlN.

The laser molecular beam epitaxy (LMBE) technique has been widely employed to prepare thin films, and the highly nonequilibrium nature of the LMBE process is desirable for the growth of metastable cubic AlN. The epitaxial growths of cubic AlN on Si (100) [5], Al_2O_3 (0001) [6], MgO (100) [7] and 3C-SiC (100) [8] have been reported. During these depositions, the crystalline plane of the substrate surface and processing conditions significantly influence the crystallinity of cubic AlN films. Since TiN (NaCl structure, $a = 0.424$ nm) has high lattice matching with cubic AlN crystallized in NaCl structure, high-quality cubic AlN films are expected to be grown on TiN templates. In this study, TiN thin films were first deposited on Si (100) substrates and then cubic AlN films were prepared on top of the TiN films by the LMBE technique under optimal conditions. The crystal structure and optical and electrical properties of the cubic AlN films were studied.

2 Experimental

The depositions were carried out in a LMBE system which can be evacuated to a base pressure of 10^{-5} Pa. Cleaned Si (100) substrates were mounted 5 cm apart from pure AlN (99.9% purity) and TiN (99.9% purity) targets. A KrF excimer laser ($\lambda = 248$ nm, $\tau = 10$ ns) with the repetition rate of 5 Hz was first focused on the TiN target under the laser pulse energy of 200 mJ and the substrate temperature of 700°C. Meanwhile, N_2 (99.999% purity) was introduced into the chamber to reach a working pressure of 10^{-3} Pa. Then, the AlN target was ablated by the laser at an energy

Y. Fu (✉) · X. Li · Y. Wang · H. He · X. Shen
Key Laboratory of New Processing Technology for Materials and Nonferrous Metals, Ministry of Education, College of Materials Science and Engineering, Guangxi University, Nanning 530004, China
e-mail: fuyuechun@126.com
Fax: +86-771-3270152

of 110 mJ/pulse and a substrate temperature of 750°C, during which the working pressure was kept at 10^{-1} Pa. The crystallinity and surface atomic structure during film depositions were characterized by in situ reflection high-energy electron diffraction (RHEED), and the typical thicknesses of AlN and TiN under study were 92 nm and 15 nm, respectively.

The crystal structures of the deposited films were characterized by X-ray diffraction (XRD) (Rigaku D/MAX-RB), scanning electron microscopy (SEM) (Hitachi S-3400N) equipped with electron-backscattered diffraction (EBSD), and Fourier transform infrared (FTIR) spectroscopy (Nexus 470) in reflection. The optical constants of the films were acquired using spectroscopic ellipsometry (SC620UVN). For the electrical measurements, Ag dots (∅4 mm) were evaporated onto the AlN films through a shadow-mask technique to realize the top electrodes for a metal–insulator–semiconductor (MIS) structure. At the back side of the substrate, an Ag film was globally deposited for the bottom electrical contact. The capacitance–voltage (C–V) features were measured using a semiconductor device analyzer (Agilent B1500A).

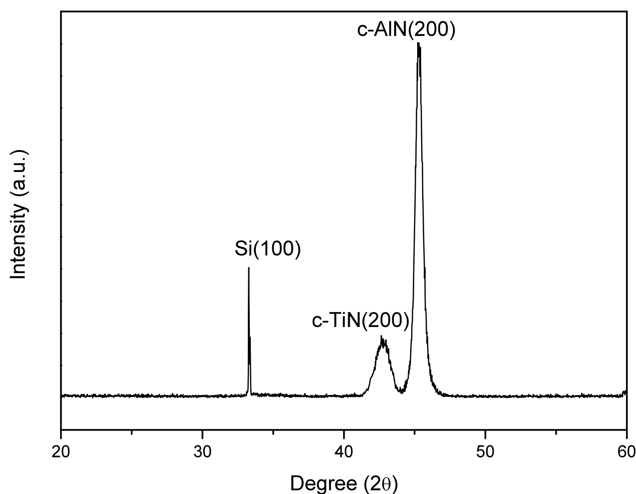

Fig. 1 The XRD pattern of AlN/TiN/Si heterostructure

3 Results and discussion

3.1 Crystal structure

The XRD pattern of the deposited films is shown in Fig. 1 and peak positions for AlN, TiN and Si substrate are labeled. For such thin thickness of the TiN film, the surface energy dictates the outcome of the film orientation, and thus the TiN film shows a (200) preferred orientation to provide the lowest overall energy. The strong peak corresponding to cubic AlN (200) with NaCl-type structure is prominent, and the lattice parameter is determined to be 0.4027 nm, which is consistent with the standard data of B1-type cubic AlN. The formation of cubic AlN film is also confirmed by the EBSD pattern as shown in Fig. 2. A single-crystal film has been detected, which is evidenced by the pole figure only exhibiting the (100) orientation. These results suggest that AlN and TiN films grow in a cube-on-cube mode, and a metastable cubic AlN film can be successfully deposited on the cubic TiN template.

During the exploring of optimal conditions to deposit cubic AlN films, we found that processing parameters (especially substrate temperature, laser energy and N_2 pressure) and the crystalline plane of the TiN films strongly influence the growth of the cubic AlN films. Generally, the surface mobility of constituent particles is enhanced with increasing laser energy and substrate temperature owing to the higher kinetic energy transferred from the bombarding particles [9]. However, at high laser pulse energy, increased number of particle collisions in the plasma may lead to high stress and point defects, and hence decrease the crystallinity and surface quality of the cubic AlN films. So, the laser pulse energy preparing cubic AlN films in the present study is lower than that of TiN films, but the substrate temperature is a little higher. N_2 introduced to the deposition chamber can make up the nitrogen deficiency in the films, and the pressure required for cubic AlN growth is higher than that for TiN, showing a similar trend with the reported literature [6]. Moreover, cubic TiN and AlN have a small lattice mismatch, and the terminating atomic layer of TiN (200) could enhance

Fig. 2 (**a**) EBSD pattern and (**b**) (001) pole figure of cubic AlN film

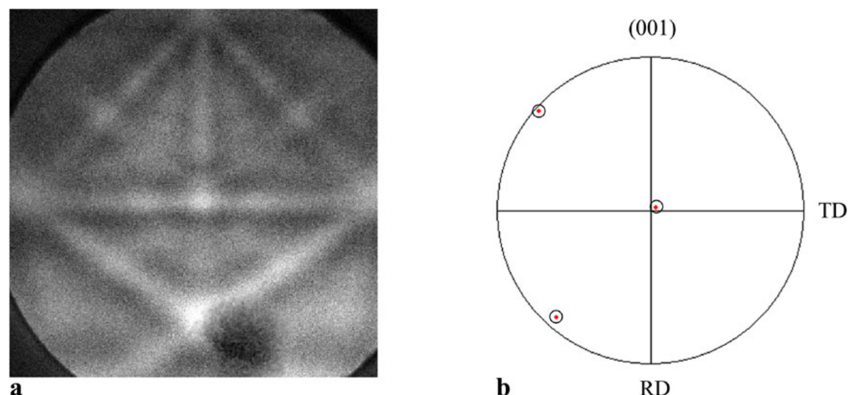

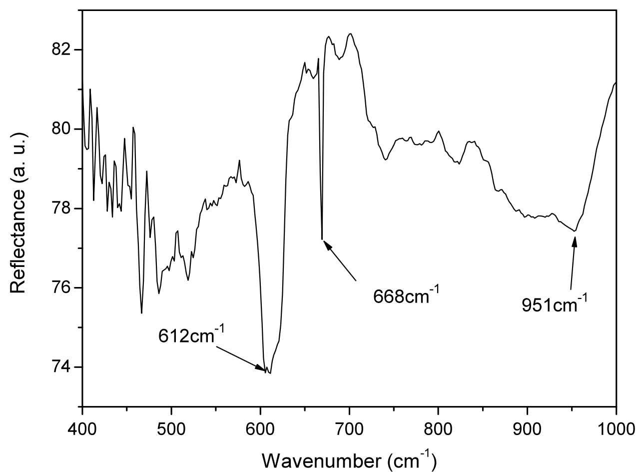

Fig. 3 The FTIR pattern of cubic AlN film

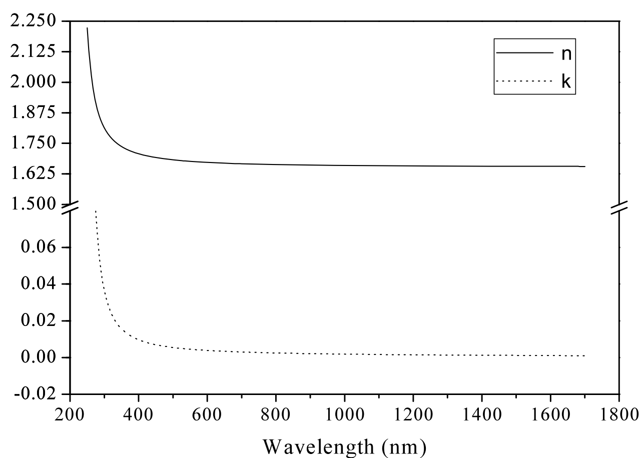

Fig. 4 Refractive index and extinction coefficient of cubic AlN film

the surface migration and nucleation of cubic AlN, and thus cubic AlN can stably exist in a wide thickness range.

Figure 3 shows the FTIR pattern of a cubic AlN film and the spectrum illustrates three obvious absorption peaks at wavenumbers of 612 cm^{-1}, 668 cm^{-1} and 951 cm^{-1}. The peak at 612 cm^{-1} is assigned to the characteristic vibration mode of Si (100) substrates [10]. Since crystalline TiN exhibits the characteristic vibration mode in the range of 565–532 cm^{-1} [10] and shows high reflectance to the infrared spectrum [11], there is no FTIR peak of TiN for the sample investigated here. Therefore, the sharp absorption peaks at 668 cm^{-1} and 951 cm^{-1} are believed to be the transverse and longitudinal optical vibration modes of cubic AlN, showing a strengthened Al–N bond. According to reported publications [5, 12], no consistent FTIR peak positions of NaCl-type cubic AlN are provided. In the present study, the peaks at 668 cm^{-1} and 951 cm^{-1} are close to those of relaxed wurtzite AlN [9, 13] though they have different phonon modes, and reasons for this may be the residual stress induced from the deposition process.

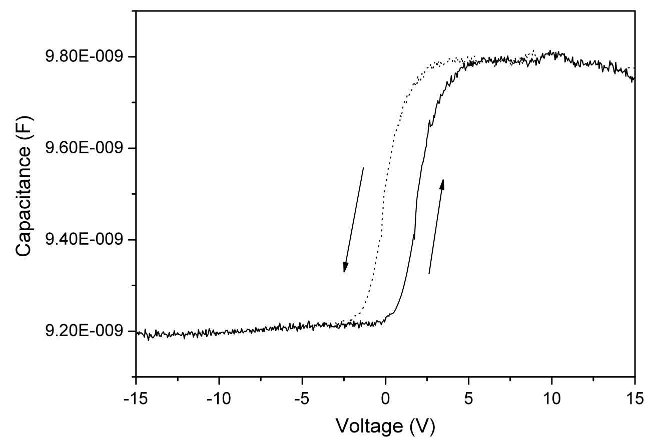

Fig. 5 C–V characteristic curves of the MIS device structure

3.2 Optical and electrical properties

Figure 4 shows the optical constants of a cubic AlN film as a function of wavelength. The refractive index (n) in the visible range is 1.66–1.71, which is lower than that of wurtzite AlN [14], but in good agreement with that of zinc-blende cubic AlN calculated by first principles [15]. In the visible and far-infrared band ($\lambda > 340$ nm), the extinction coefficient (k) approaches zero, but increases rapidly in the near-ultraviolet band, showing a strong absorption characteristic.

The C–V characteristics of the MIS structure at a frequency of 1 MHz are shown in Fig. 5. The solid and dotted lines indicate different sweep directions. Three regions of the C–V curve, namely accumulation, depletion and inversion, due to the variation in carrier concentrations at the interface with bias voltage, are distinctly visible. The flat-band voltage exhibits a positive shift, indicating the existence of negative charges trapped in the cubic AlN/Si interface. For the present MIS structure, the thin TiN film showing metallic conduction lies between the cubic AlN film and the Si substrate, and thus the hysteresis occurs due to mobile charges of TiN in the interface.

In accumulation, the maximum capacitance, C_{max}, of the film can be obtained directly, and the dielectric constant of the film can be calculated from $C_{max} = \varepsilon\varepsilon_0 A/d$, where A is the area of the MIS device, d is the thickness of the AlN layer and ε_0 is the permittivity of free space. Using this relationship, the dielectric constant of the cubic AlN film investigated here is 8.1, comparable to that of zinc-blende cubic AlN determined by ellipsometry [8].

4 Conclusions

Highly oriented cubic AlN films with NaCl-type structure were successfully deposited on TiN-buffered Si (100) substrates using the LMBE technique. At optimal processing

conditions, cubic AlN shows a (200) preferred orientation with the lattice parameter a of 0.4027 nm. The FTIR pattern of the cubic AlN film shows a strengthened Al–N bond evidenced by the sharp absorption peaks at 668 cm^{-1} and 951 cm^{-1}. The refractive index of cubic AlN in the visible range is 1.66–1.71, and the extinction coefficient approaches zero in the visible and far-infrared band. For the MIS structure, the C–V traces indicate that the cubic AlN film has a dielectric constant of 8.1, and the hysteresis occurs due to mobile charges of TiN in the cubic AlN/Si interface.

Acknowledgements This work was financially supported by the Open Foundation of the Key Laboratory of New Processing Technology for Nonferrous Metals and Materials (No. GXKFZ-05) and the Guangxi High Education Scientific Research Project (No. 200103YB003).

References

1. I. Petrov, E. Mojab, R.C. Powell, J.E. Greene, L. Hultman, J.E. Sundgren, Appl. Phys. Lett. **60**, 2491 (1992)
2. M.P. Thompson, G.W. Auner, A.R. Drews, J. Electron. Mater. **10**, L17 (1999)
3. L.D. Wang, H.S. Kwok, Appl. Surf. Sci. **154–155**, 439 (2000)
4. M. Shahien, M. Yamada, T. Yasui, M. Fukumoto, J. Therm. Spray Technol. **19**, 635 (2010)
5. Z.M. Ren, Y.F. Lu, H.Q. Ni, J. Appl. Phys. **88**, 7346 (2000)
6. S. Mohri, T. Yoshitake, T. Hara, K. Nagayama, Diam. Relat. Mater. **17**, 1796 (2008)
7. S. Okubo, N. Shibata, T. Saito, Y. Ikuhara, J. Cryst. Growth **189–190**, 452 (1998)
8. M. Röppischer, R. Goldhahn, G. Rossbach, P. Schley, C. Cobet, N. Esser, T. Schupp, K. Lischka, D.J. As, J. Appl. Phys. **106**, 076104 (2009)
9. G. Shukla, A. Khare, Appl. Surf. Sci. **255**, 2057 (2008)
10. Y.K. Ke, H.R. Dong, *Handbook of Chemical Analysis* (Chemical Industry Press, Beijing, 1998)
11. L.I. Wei, C.J. Fang, Appl. Surf. Sci. **253**, 7019 (2007)
12. M. Bernard, A. Deneuville, O. Thomas, P. Gergaud, P. Sandstrom, J. Birch, Thin Solid Films **380**, 252 (2000)
13. C. Ristoscu, C. Ducu, G. Socol, F. Craciunoiu, I.N. Mihailescu, Appl. Surf. Sci. **248**, 411 (2005)
14. J. Baek, J. Ma, M.F. Becker, J.W. Keto, D. Kovar, Thin Solid Films **515**, 7096 (2007)
15. P.E. Silva, P.R. De, L.C. Carvalho, Microelectron. J. **34**, 721 (2003)